Cyclin D2 in the basal process of neural progenitors is linked to non-equivalent cell fates

Yuji Tsunekawa[1], Joanne M Britto[2], Masanori Takahashi[1], Franck Polleux[3], Seong-Seng Tan[2] and Noriko Osumi[1],*

[1]Division of Developmental Neuroscience, United Core Centers for Advanced Research and Translational Medicine, Tohoku University Graduate School of Medicine, Sendai, Japan, [2]Brain Development and Regeneration Laboratory, Florey Neuroscience Institutes, University of Melbourne, Melbourne, Victoria, Australia and [3]Department of Cell Biology, Dorris Neuroscience Center, The Scripps Research Institute, La Jolla, CA, USA

Asymmetric cell division plays an indispensable role during corticogenesis for producing new neurons while maintaining a self-renewing pool of apical progenitors. The cellular and molecular determinants favouring asymmetric division are not completely understood. Here, we identify a novel mechanism for generating cellular asymmetry through the active transportation and local translation of *Cyclin D2* mRNA in the basal process. This process is regulated by a unique *cis*-regulatory sequence found in the 3′ untranslated region (3′UTR) of the mRNA. Unequal inheritance of Cyclin D2 protein to the basally positioned daughter cell with the basal process confers renewal of the apical progenitor after asymmetric division. Conversely, depletion of Cyclin D2 in the apically positioned daughter cell results in terminal neuronal differentiation. We demonstrate that Cyclin D2 is also expressed in the developing human cortex within similar domains, thus indicating that its role as a fate determinant is ancient and conserved.

Introduction

During cortical development in mammals, the expansion of the cortical wall relies on large numbers of neurons to be generated by proliferating neuroepithelial cells (Smart, 1973). At early stages of corticogenesis (embryonic day 10.5 (E10.5)), these neuroepithelial cells divide symmetrically to yield more progenitors, resulting in a thickened pseudostratified sheet where the mitotic cells are concentrated mainly

*Corresponding author. Division of Developmental Neuroscience, United Core Centers for Advanced Research and Translational Medicine, Tohoku University School of Medicine, 2-1 Seiryo-machi, Aoba-ku, Sendai 980-8575, Japan. Tel.: +81 22 717 8201; Fax: +81 22 717 8205; E-mail: osumi@med.tohoku.ac.jp

on the apical side of the epithelium (Rakic, 1988). The dividing cells attached to the apical membrane are called apical progenitors (APs), and during the proliferative stage they undergo mostly symmetric cell divisions, producing daughter cells with equal fates (as neurons or more progenitors) (Huttner and Kosodo, 2005). Later in corticogenesis (E12.5–15.5), neuroepithelial cells become radial glia and start to divide asymmetrically, producing an AP with self-renewing capacity together with a terminally differentiated neuron or intermediate progenitor (IP) (Gotz and Huttner, 2005). Newly produced neurons migrate out of the ventricular zone (VZ) to form the cortical plate (CP), while intermediate progenitors divide symmetrically in the subventricular zone (SVZ) and generate more IPs or neurons (Haubensak *et al*, 2004; Miyata *et al*, 2004; Noctor *et al*, 2004). APs undergoing symmetric and asymmetric divisions often overlap and coexist in the germinal zones (Huttner and Kosodo, 2005), but what is unclear is the motivation driving symmetric versus asymmetric divisions (Gotz and Huttner, 2005).

Asymmetric cell division of neural progenitor cells is critical for establishing the architectures of the mammalian cerebral cortex by regulating the balance between proliferative and neurogenic populations. This is achieved by producing daughter cells that are self-renewing together with daughter cells that become postmitotic neurons and thereby increasing the number of neurons while maintaining the number of APs (Gotz and Huttner, 2005; Kriegstein *et al*, 2006). In addition, asymmetric cell division is capable of generating a third class of offspring known as the intermediate progenitor whose cell body lies in the SVZ and retracts its apical attachment prior to mitosis (Miyata *et al*, 2004; Attardo *et al*, 2008). These observations invite the question—what cellular factors influence mitotic descendants to become a self-renewing AP or a differentiated neuron?

A key issue in this debate concerns the roles played by structural elements such as the apical membrane or basal process, and their cytoplasmic constituents, in conferring AP fate. The cleavage plane *per se* is not an indicator of symmetric or asymmetric division (Kosodo *et al*, 2004), but experimental randomization of the cleavage plane (by changing mitotic spindle orientation) decreases the number of APs (Konno *et al*, 2008). Leaving cleavage plane aside, it has been suggested that asymmetric inheritance of fate-determining constituents present in the apical process is sufficient to ensure asymmetric division (Kosodo *et al*, 2004; Attardo *et al*, 2008; Bultje *et al*, 2009), but this notion has been undermined by a recent study showing that even complete inheritance of the apical process is no guarantor of AP fates (Konno *et al*, 2008). In this context, the status of the basal process has been underexplored, although it has been hypothesized that inheritance of both apical and basal processes is required for self-renewing capability (Konno *et al*, 2008). Certainly, basal process splitting has been observed to accompany both symmetric and asymmetric neuroepithelial

divisions (Kosodo *et al*, 2008; Kosodo and Huttner, 2009), although there is controversy whether asymmetric inheritance of the basal process is predictive of neuronal differentiation (Miyata *et al*, 2001) or progenitor renewal (Ochiai *et al*, 2009; Alexandre *et al*, 2010).

In the current study, we set out to explore the role of the basal process, in particular the contribution by the polarized distribution of Cyclin D2, in the determination of apical progenitor fate. Previous studies have established that Cyclin D2 protein localized in the basal process of neural progenitors (Glickstein *et al*, 2007), and as a member of the Cyclin family, may be involved in the regulation of the cell cycle (Dehay and Kennedy, 2007; Salomoni and Calegari, 2010). Other studies have established that another family member, Cyclin D1, is implicated in regulating the balance between the number of cortical cells undergoing proliferation or becoming IPs (Lange *et al*, 2009). Here, we demonstrate using mouse cortical tissue the polarized distribution of *Cyclin D2* mRNA and protein in neural progenitors. We identify a novel 50 base pair (bp) *cis*-acting transport element for the basal localization of *Cyclin D2* mRNA within its 3′ untranslated region (3′UTR) and showed that *Cyclin D2* mRNA is locally translated into protein at the basal endfoot. We provide several lines of evidence to suggest that post-transcriptional regulatory systems are required for asymmetric segregation of Cyclin D2 protein to one of the two daughter cells. In addition, gain- and loss-of-function experiments that perturb asymmetrical distribution of Cyclin D2 protein in apical progenitor cells severely distort asymmetry of the cell fate. Finally, we show that protein localization of Cyclin D2 is highly conserved in the human fetal cortex. Taken together, we propose a model for Cyclin D2 as a fate determinant by the asymmetrical distribution of Cyclin D2 to the basal process and subsequent inheritance to the mitotic offspring with self-renewing capacity.

Results

Localization patterns of Cyclin D2 mRNA and protein during early corticogenesis

Localization of Cyclin D2 protein in the developing neocortex has been previously reported (Ross *et al*, 1996; Glickstein *et al*, 2007), while detailed subcellular distributions with regard to developmental periods and cell-cycle phases have not been elucidated. We first examined changes in the expression patterns of *Cyclin D2* mRNA and protein in mouse forebrain during the proliferation (E10.5) and neurogenic stages (E14.5). Antibody specificity was confirmed by western blotting and immunostaining on *Cyclin D2* knockout mouse neocortex with wild-type littermates (Supplementary Figure S1).

From E10.5 to E14.5, *Cyclin D2* mRNA was detected in the cortical wall, mostly near the basal lamina as reported by others, and weakly in the VZ (Figure 1A–C). In comparison, mRNA of another members of the Cyclin family, *Cyclin D1* and *Cyclin D3*, was present in the VZ but not at the basal edge of the cortical primordium (Supplementary Figure S2). At higher magnification, expression of *Cyclin D2* mRNA and protein in the cortical wall showed unique and differential patterns. *Cyclin D2* mRNA was preferentially localized in subcellular structures adjacent to the basal lamina at all three stages examined (Figure 1D, F and H). On the other hand, the protein was evenly distributed in cellular nuclei of

the epithelial sheet at E10.5 (Figure 1E), but at older stages (E12.5 and 14.5) the protein showed a dual distribution pattern directed at basal processes and VZ cells with little staining in between (Figure 1G and I). At these stages, Cyclin D2 protein in the VZ and SVZ was found in the nucleus (arrow in inset of Figure 1G), although not all cells were immunopositive (double arrow in inset of Figure 1G). Even though Cyclin D2 protein was expressed in nuclear and non-nuclear compartments, *Cyclin D2* mRNA itself was consistently found in cytoplasmic structures on the basal but not apical aspects of the neuroepithelium.

To confirm *Cyclin D2* mRNA and protein were expressed in neural progenitor cells, fluoro *in-situ* hybridization with immunostaining and double immunostaining of *Cyclin D2* mRNA and protein with βIII-tubulin (which marks neurons) was performed in the E12.5 cortex. The results show that *Cyclin D2* mRNA and protein localization in basal structures was essentially non-neuronal (Figure 1J and K, arrowheads). Instead, double immunocytochemistry with laminin indicates that Cyclin D2 staining was not coextensive with the basement membrane (Figure 1L), but restricted in the basal endfoot of neuroepithelial cells revealed by EGFP-lentiviral reporter (Figure 1M and N). Thus, polarized Cyclin D2 expression in the basal processes of neural progenitors appears during the onset of neurogenesis, and is maintained thereafter.

A cis-acting transport element of Cyclin D2 mRNA resides in its 3′UTR

To elucidate the mechanism behind the polarized distribution of *Cyclin D2* mRNA in cortical progenitor cells, whole-embryo cultures and electroporation experiments were conducted (Supplementary Figure S3A; Osumi and Inoue, 2001). Since localization of mRNA is usually achieved by the binding of a *cis*-acting transport element with a *trans*-acting localization factor (Palacios and St Johnston, 2001), we tested whether a *cis*-acting transport element is present in the 3′UTR of *Cyclin D2* (AK147345). A reporter construct, *pCE/CD2/3′*, was generated by inserting the entire 3′UTR region of *Cyclin D2* mRNA (1106–6274) into an open reading frame (ORF) downstream of *EGFP* in pCAX. This construct was co-electroporated with *pCAGGS-mRFP* into the diencephalon of E12.5 embryos, which were subsequently cultured for 12 h (Supplementary Figure S3A). Localization of transcribed mRNAs was detected by *in-situ* hybridization using *EGFP* and *mRFP* riboprobes on adjacent sections from electroporated embryos. The results demonstrate that *EGFP* mRNA fused with a *Cyclin D2* 3′UTR sequence was distributed both in the VZ and in the basal endfoot of neural progenitor cells (Figure 2A), while *mRFP* mRNA without a *Cyclin D2* 3′UTR sequence was present only in the VZ (Figure 2B). This suggests that a *cis*-acting transport element of *Cyclin D2* mRNA is present in its 3′UTR region and is capable of transporting reporter mRNA into the basal endfeet. The speed of this transport event (distance of 400 μm in the basal process within 12 h) suggests that passive diffusion or lack of mRNA degradation is unlikely to account for the observed polarized distribution of *Cyclin D2* mRNA. Further characterization of this sequence by the use of truncated fragments of the *Cyclin D2* 3′UTR yielded a minimal 50 bp element (*pCE/CD2/3′/3965-4015*) that was sufficient for basal localization of *Cyclin D2* mRNA, both in the diencephalon and in the cortex (Figure 2C and D;
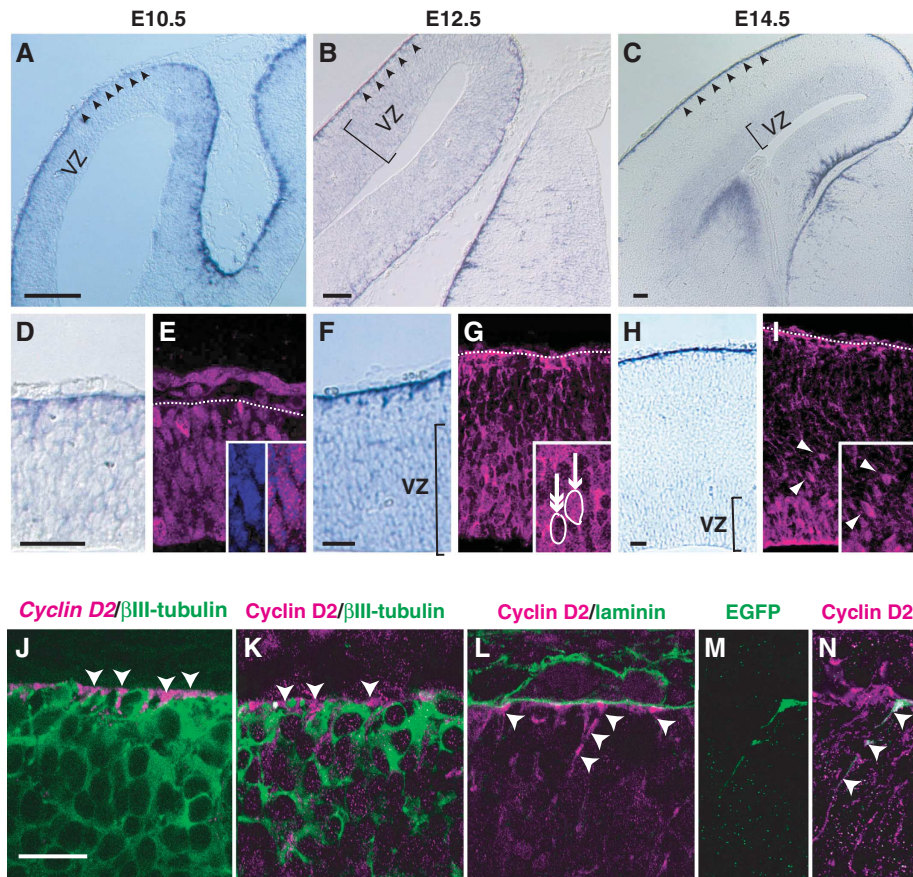
Figure 1 Expression patterns of *Cyclin D2* mRNA and protein during cortical development. (**A–I**) Localization of *Cyclin D2* mRNA and protein in sections from mouse embryonic neocortex demonstrated by *in-situ* hybridization and immunostaining. At E10.5, *Cyclin D2* mRNA is mainly observed at the basal edge of the neuroepithelium (arrowheads in **A**, higher magnification in **D**), whereas Cyclin D2 protein appears to be uniformly distributed in the nuclei across the epithelial sheet (inset in **E**). At E12.5 and E14.5, *Cyclin D2* mRNA is preferentially expressed on the basal side of radial glia including the basement membrane (**F**, **H**). In contrast, Cyclin D2 protein is strongly expressed in structures next to the basal lamina (**G**, **I**), as well as in the VZ where cells showing strong nuclear staining (inset in **G**, arrow) are situated next to other cells devoid of Cyclin D2 protein (inset in **G**, double arrows). A similar distribution pattern is observed at E14.5 with the additional observation that SVZ cells contain Cyclin D2 protein (**I**, arrowheads). (**J–L**) Double immunostaining in E12.5 cortex shows that *Cyclin D2* mRNA (**J**) and protein (**K**) is found in basal endfeet of non-neuronal processes identified by the lack of βIII-tubulin (**J** and **K**, arrowheads). Cyclin D2 protein is detected in the apical side of the basal lamina revealed by laminin immunoreactivity (arrowheads in **L**), and also in the basal process and endfoot of radial glia revealed by EGFP-lentiviral infection (**M** and **N**, arrowheads). Dotted lines denote the location of the basal lamina, VZ, ventricular zone. Scale bars: 100 μm in (**A–C**), 50 μm in (**D–I**), and 20 μm in (**J–N**).

Supplementary Figure S3B and C). This finding indicates that a 3′UTR transport element regulates the active transport of *Cyclin D2* mRNA to the basal endfoot.

Transported Cyclin D2 mRNA is translated locally in the basal endfoot

To examine whether the *Cyclin D2* mRNA in the basal endfeet is translated *in situ*, an expression vector, *pCEN/CD2/3′/1496-5457*, containing EGFP with a nuclear localization signal (NLS-EGFP) was electroporated together with *pCAGGS-mRFP* into E13.5 forebrain *in utero* (Takahashi *et al*, 2002; Figure 3A). A construct containing Cyclin D2 3′UTR nucleotides 1496–5457 placed downstream of NLS-EGFP in a reverse direction (*pCEN/CD2/3′/5457-1496*) was used as a control for these experiments (Figure 3A). Following fixation 24 h later, *NLS-EGFP* mRNA linked to *Cyclin D2* 3′UTR (1496–5457) was observed at the basal endfoot (Figure 3B and B'), while the control mRNA was located only at the VZ with no

polarized distribution to the basal endfeet (Figure 3E and E'). At the protein level, EGFP translated from *pCEN/CD2/3′/1496-5457* was present at the basal endfeet and ventricular nuclei (Figure 3C and C'), whereas EGFP translated from *pCEN/CD2/3′/5457-1496* was present only in nuclei but undetected in the basal endfeet (Figure 3F and F'). From this line of investigation, we predicted that the translated EGFP would be immediately transported into the nucleus via its NLS. However, this is not the case and localization was also noted in the basal endfoot. It has been reported that translation systems, such as ribosomes, are localized at the basal endfoot of the neural progenitor cells (Astrom and Webster, 1991); and therefore, we can conclude that the EGFP observed at the basal endfoot is locally translated and driven by the presence of the *Cyclin D2* 3′UTR. Co-expressed mRFP was seen in the basal processes and basal endfeet, confirming visible observation of the reporter in the endfeet (Figure 3D, D', G, and G').
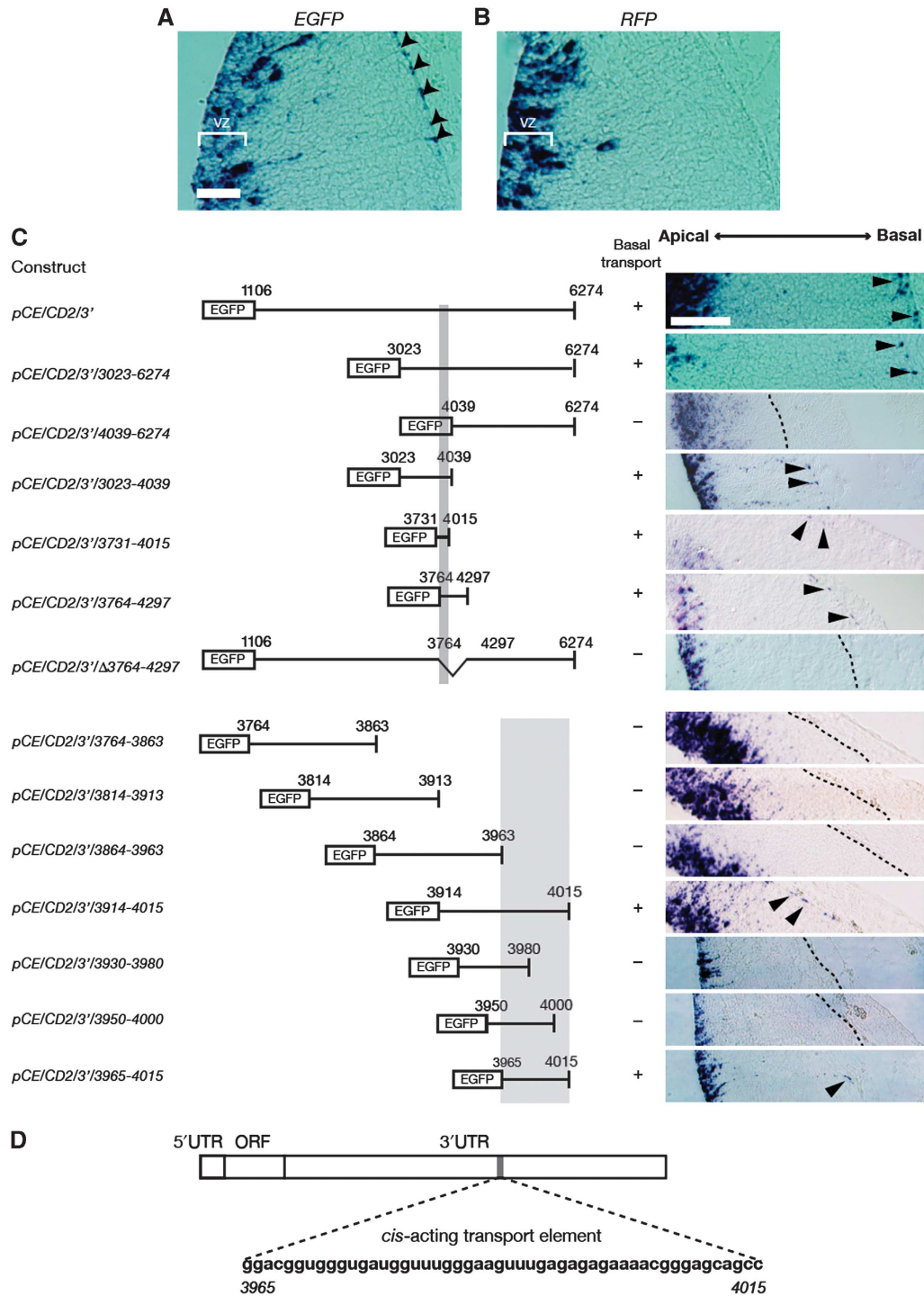
Figure 2 *Cyclin D2* mRNA contains a *cis*-acting transport element in the 3′ untranslated region. *In-situ* hybridization for *EGFP* (**A**) and *RFP* mRNA (**B**), coded by *pCE/CD2/3′* and *pCAGGS-mRFP*, respectively, following electroporation at E12.5. *EGFP* mRNA is found in the VZ as well as in the basal process and the basal endfoot of the radial glia (arrowheads in **A**). In contrast, *RFP* mRNA without *Cyclin D2* 3′UTR is only found in the VZ without expression in the basal process (**B**). (**C**) Identification of a 50 nucleotide *cis*-acting mRNA transport element in the *Cyclin D2* 3′ UTR. Left panel, regions of the *Cyclin D2* 3′ UTR fused with *EGFP* ORF, right panel shows localization of *EGFP-CyclinD2 3′UTR* chimeric mRNA in the mouse diencephalon. (**D**) Diagrammatic representation of *Cyclin D2* mRNA and *cis*-acting transport element (3965–4015). VZ, ventricular zone. Scale bar: 100 µm.

Cyclin D2 protein is asymmetrically inherited by one of the two daughter cells

During asymmetric progenitor division, the basal process is inherited by one of its two daughter cells (Miyata *et al*, 2001; Noctor *et al*, 2001). This poses the question of whether the Cyclin D2 protein is also asymmetrically inherited, and if so,

to which daughter cell does the Cyclin D2-containing basal process belong to? To address this, Cyclin D2 protein was analysed in the basal process and cell body of mitotic off-spring revealed by EGFP-lentiviral infection of E11.5 embryos examined 24 h later. The viral titre used was sufficiently low to produce an infected clone (with 1–3 cells) per cortical
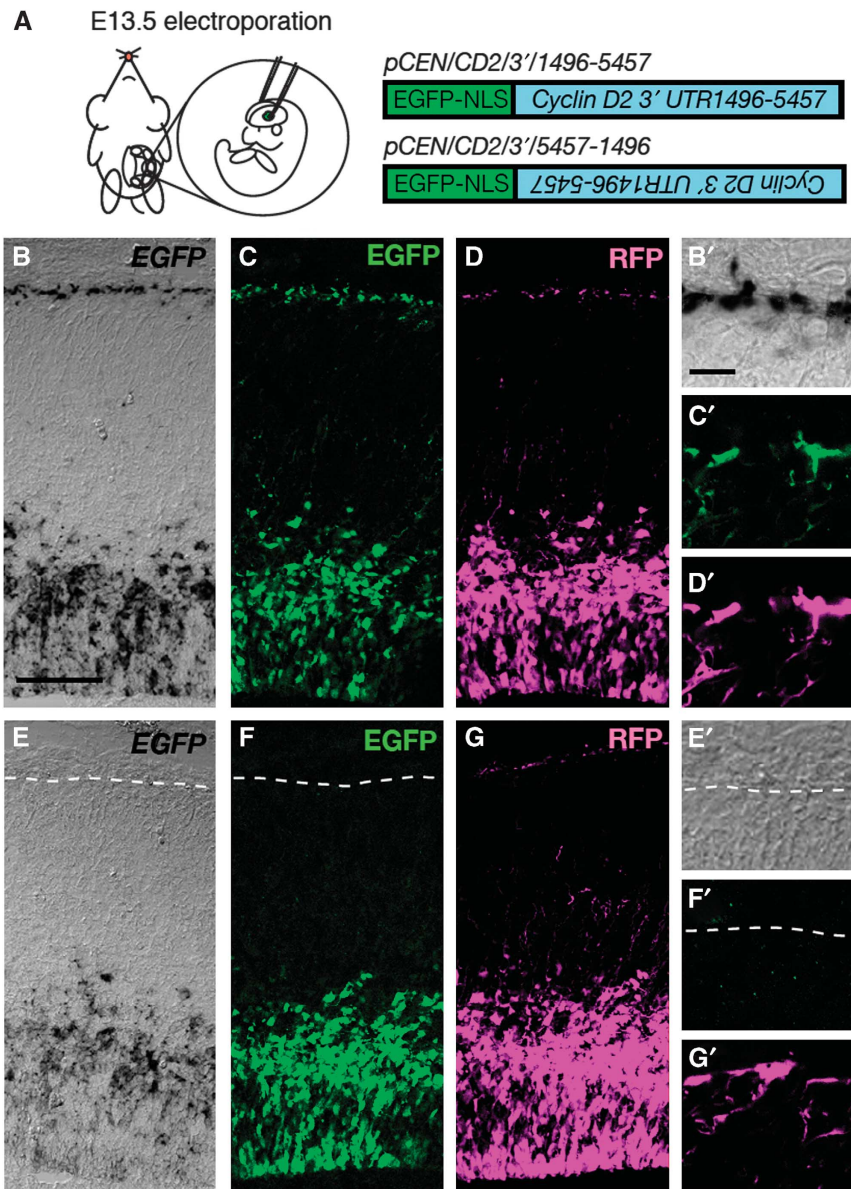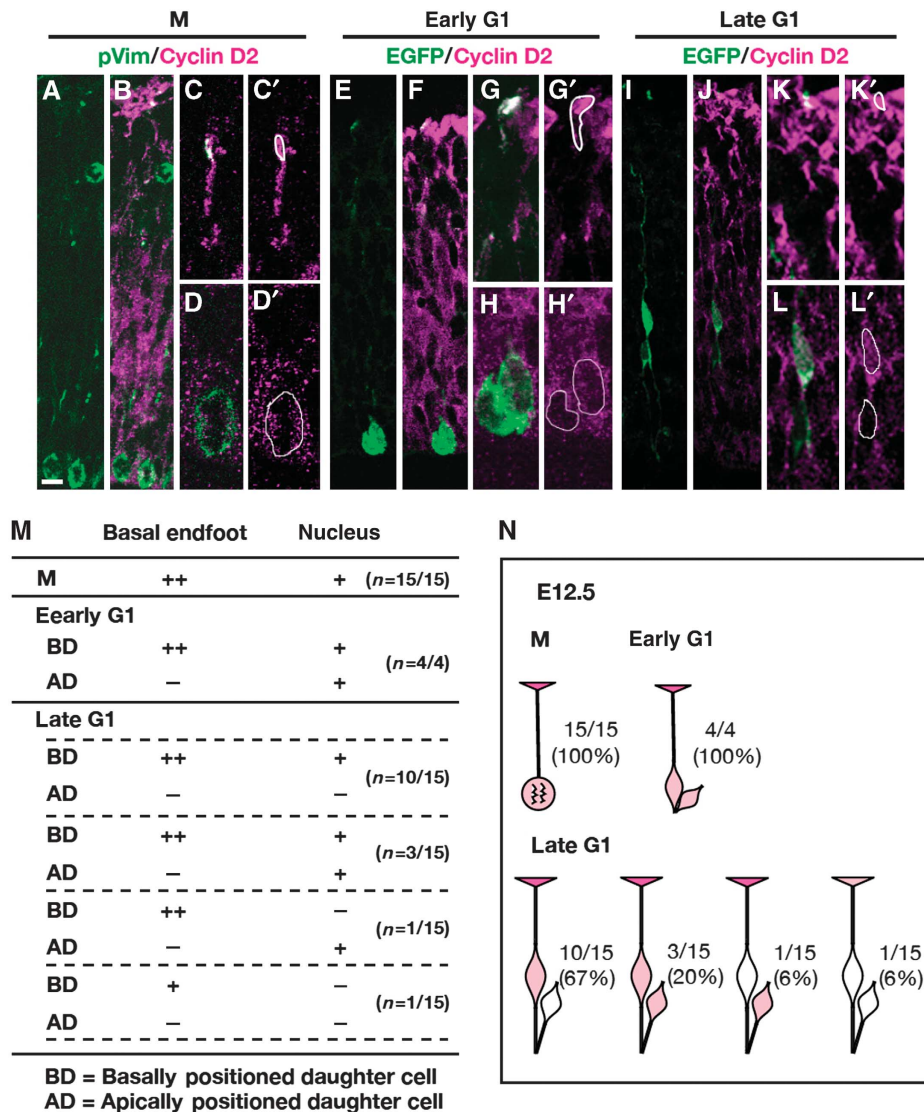
Figure 3 Reporter mRNAs carrying *Cyclin D2* 3′UTR transport element are directed to the basal endfeet and translated locally. (**A**) EGFP constructs carrying Cyclin D2 transport element in forward and reverse orientation (*pCEN/CD2/3′/1496-5457* and *pCEN/CD2/3′/5457-1496*) were introduced into the E13.5 mouse neocortex by *in-utero* electroporation, together with *pCAGGS-mRFP*. (**B–G**) Analysis 24 h later shows that mRNA for EGFP, from *pCEN/CD2/3′/1496-5457*, is expressed at the basal endfeet of radial glia (**B** and **B'**). Conversely, *EGFP* mRNA from *pCEN/CD2/3′/5457-1496* is absent from the basal endfeet (**E** and **E'**). At the protein level, EGFP translated from *pCEN/CD2/3′/1496-5457* is present at the basal endfoot and VZ cells (**C** and **C'**), whereas EGFP from the reversed *pCEN/CD2/3′/5457-1496* is present only in the VZ but undetected in the basal endfoot (**F** and **F'**). Co-transfection with RFP indicates that the reporter protein can be visibly observed in the basal processes and endfeet (**D**, **D'**, **G** and **G'**). Scale bars: 100 μm in (**B–G**) and 10 μm in (**B'–G'**).

hemisphere, or neighbouring clusters with sufficient separation to be considered as clonal (refer to Supplementary Figure S4). To clearly identify the progenitor cell with its attached basal process, we performed three-dimensional reconstruction of individual daughter cells using Z-stacked images ($n = 28$) (a representative image is shown in Supplementary Movie 1). This analysis has revealed that most of the basal processes are inherited by basally positioned daughter cells (26/28) as previously reported (Ochiai *et al*, 2009).

A transfection protocol was employed to express EGFP in the basal process and immunostaining for Cyclin D2 was

conducted to detect protein distribution at different stages of the cell cycle (Figure 4). Cells in M phase were identified using an antibody against phospho-Vimentin (pVim) that stains M-phase cytoplasm and the basal fibres (Figure 4A; Kamei *et al*, 1998). At the M phase ($n = 15$), Cyclin D2 was weakly expressed in the nucleus but strongly expressed in the basal process and endfoot (Figure 4A–D, M, and N). Thus, Cyclin D2 is continuously present in the basal endfoot of APs during the M phase.

To analyse early G1 to late G1 phase, 22 embryos at E12.5 were transfected with the reporter GFP vector. This yielded 19 daughter pairs sharing a single apical process and one basal

M	Basal endfoot	Nucleus	
M	++	+	(n=15/15)
Eearly G1			
BD	++	+	
AD	−	+	(n=4/4)
Late G1			
BD	++	+	
AD	−	−	(n=10/15)
BD	++	+	
AD	−	+	(n=3/15)
BD	++	−	
AD	−	+	(n=1/15)
BD	+	−	
AD	−	−	(n=1/15)

BD = Basally positioned daughter cell
AD = Apically positioned daughter cell

Figure 4 Location and inheritance of Cyclin D2 protein by clonal pairs during the cell cycle at E12.5 using an EGFP lentivirus. (A–D') Identification of clones containing phospho-vimentin-positive M cells show weak Cyclin D2 distribution in the nucleus and basal endfoot. (E–H') A single clone-derived pair of daughter cells anchored by an apical membrane were considered to be in early G1. (G, H') are high-magnification images of centrally positioned cell body and a basal endfoot shown in (C). Cyclin D2 protein at this stage is present in the basal process attached to the basally positioned daughter whose nucleus is also stained for Cyclin D2. The apically positioned daughter is weakly positive for Cyclin D2. (I–L') At late G1, Cyclin D2 is clearly expressed in the basal process and endfoot belonging to the basally positioned daughter (also stained for Cyclin D2). In contrast, the apically positioned daughter is devoid of Cyclin D2. (M) Summary of Cyclin D2 expression in the basal endfoot and nucleus in cells undergoing different stages of the cell cycle. (N) Schematic diagram of Cyclin D2 expression in the basal endfoot and nucleus at different cell-cycle stages. After asymmetric cell division, the majority (67%) of offspring in late G1 shows preferential staining of Cyclin D2 in the basal endfoot and nucleus belonging to the basally positioned daughter. Intensity of the staining is shown as + (modest) and ++ (strong). Scale bar: 10 μm.

process inherited by one of the daughter cells and had therefore undergone asymmetric division (Figure 4E–N). To identify early G1 daughter pairs (n = 4), we used the criterion of close proximity of the daughter cell body to the apical surface (Ochiai *et al*, 2009), and considered these daughter cells to have been born within a 0–3 h period if one of the two daughters was still anchored to the apical membrane (Figure 4E–H'). This analysis revealed that Cyclin D2 was only weakly expressed in both daughter cell bodies (Figure 4H, H', M, and N), but strongly expressed at the basal process and endfoot (Figure 4G, G', M, and N). By contrast, cells considered to be in late G1 (born greater than 3 h ago and no longer attached to the apical membrane) (n = 15) showed four dif-

ferent patterns of Cyclin D2 inheritance (Figure 4I–N). In the majority pattern (67%; 10/15), stronger expression of Cyclin D2 was detected in the basally positioned daughter that also carried the basal process stained with Cyclin D2 in the endfoot (Figure 4M and N). Twenty percent of the pairs (3/15) showed equal expression of Cyclin D2 in both daughter cells, and one pair (6%) showed no expression Cyclin D2 in both daughter cells (Figure 4M and N). Finally, another pair (6%) displayed the opposite trend, with strong Cyclin D2 expression in the basal endfoot but no staining in its associated cell body, while the sister cell body without the basal process possessed Cyclin D2 (Figure 4M and N). Thus, Cyclin D2 presents in the basal process and endfoot during cell division, and after asymmetric

cell division, Cyclin D2 is more frequently segregated to the nucleus of the basally positioned daughter cell.

To further examine Cyclin D2 protein inheritance at later stages of neurogenesis (E14.5), E12.5 forebrains were infected with low titre EGFP lentivirus and sacrificed 48 h later (Supplementary Figure S4). Analysis of daughter pairs at early G1 (and therefore closer to the ventricle) showed a variable yet robust result, with 44% of the pairs (4/9) accumulating Cyclin D2 in the basally positioned daughter cell, while the remainder (5/9) showed no detectable Cyclin D2 expression in both daughter cells (Figure 5A–C'' and M). Daughter pairs considered to have undergone division >3 h prior to collection and situated at some distance from the apical membrane were considered to be in late G1. This analysis indicated that 100% of the late G1 daughter pairs (20/20) accumulated more Cyclin D2 protein in the basally positioned daughters (Figure 5D–F'' and M). In summary, these experiments are instructive regarding Cyclin D2 inheritance to daughter cells following apical progenitor divisions during early and mid neurogenesis. Interestingly, compared with earlier stages (E12.5; Figure 4N) a larger proportion of cells at late G1 inherited Cyclin D2 only in the basally

positioned daughter (E14.5; Figure 5M). Taken together, this retrospective staining for Cyclin D2 suggests that preferential distribution of Cyclin D2 protein to one daughter cell is strongly associated with the acquisition of dissimilar daughter cell fates.

Previous studies suggest that apically positioned daughter cells acquire postmitotic neuronal characteristics, while basally positioned daughters tend to be self-renewing (Noctor *et al*, 2001; Konno *et al*, 2008; Ochiai *et al*, 2009). To test this, Ngn2, a marker for neuronal differentiation was used to examine Cyclin D2 inheritance patterns. At E12.5, all the daughter pairs (8/8) at early G1 were devoid of Ngn2 (Supplementary Figure S5A—C and G), a trend also observed at E14.5 (Figure 5G–I'' and N). In contrast to Cyclin D2, 50% of late G1 daughter pairs (9/18) showed Ngn2 accumulation in the apically positioned daughter cell at E12.5 (Supplementary Figure S5D–F and G), and 75% of pairs (12/6) at E14 (Figure 5J–L'' and N). Together, these results strongly point to the conclusion that by late G1, a consequence of asymmetric division is the differential allocation of Cyclin D2 to the nucleus and basal process of the basally positioned daughter cell that is known to undergo self-renewal. In con-
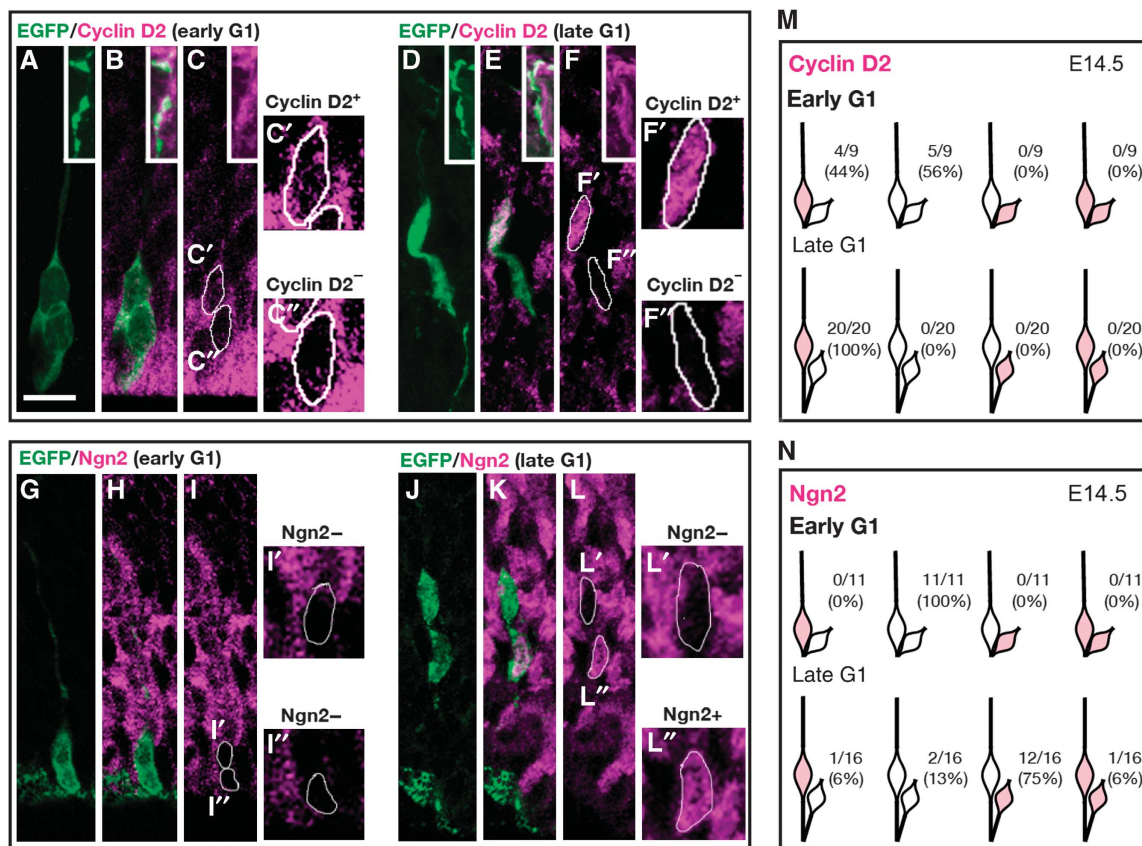
Figure 5 Cyclin D2 protein is asymmetrically inherited by basally positioned daughter cells. (**A–C''**) Daughter pairs at early G1 (<3 h after mitosis) labelled by EGFP lentivirus at E12.5 and examined at E14.5, inset in (**A–F**) shows Cyclin D2-positive basal process of radial glia. Higher magnification images (**C'** and **C''**) showing preferential allocation of Cyclin D2 to the basally positioned daughter (**C'**) while the apically positioned daughter (**C''**) is relatively empty of Cyclin D2. Strong expression of Cyclin D2 at the apical side indicates the process of other radial glial cells. (**G–I''**) At early G1 stage of the cell cycle, Ngn2 was not found in either of the two daughter cells (**I'** and **I''**). (**D–F''**) At late G1 (>3 h after mitosis), daughter pairs positioned next to the apical membrane show preferentially staining of Cyclin D2 in the basally positioned daughter cell (**F** and **F'**). In contrast, staining for the neuronal marker Ngn2 in a comparable cluster of late G1 daughters (**J–L''**) demonstrate that Ngn2 is preferentially expressed in the apically positioned daughter (**L** and **L''**). (**M**) Schematic diagram cataloguing the inheritance pattern of Cyclin D2 in late G1 (top row) and early G1 (bottom row). (**N**) Schematic diagram demonstrating Ngn2 expression in the apically positioned daughter cell in the majority (75%) of late G1 daughter pairs (top row). At early G1, Ngn2 marker is undetectable in either of the daughter cells (bottom row). Scale bar: 10 μm.

trast, by late G1 Cyclin D2 is invariably absent from the apically position daughter cell; these daughter cells acquire Ngn2 in most instances indicating terminal differentiation.

To discount the possibility that asymmetric Cyclin D2 distribution may have arisen from other causes apart from inheritance of locally translated mRNA, two further experiments were performed. The first experiment was to exclude that Cyclin D2 protein may have congregated to one side of the nucleus during M phase, resulting in subsequent asymmetry following division. To check this possibility, E14.5 M-phase neural progenitor cells were double stained with anti-pVim and anti-Cyclin D2 antibodies. The results show that Cyclin D2 protein was only weakly expressed in the nucleus during M phase, and in no case was the distribution asymmetric ($n = 32$) (Supplementary Figure S6A–C). The second possibility is that one of the daughter cells committed for self-renewability may transcribe and translate Cyclin D2 *de novo*. If this is the case, then one of the two daughter cells should exhibit a higher level of *Cyclin D2* mRNA. This was not seen in daughter cells labelled with lentiviral infection and stained for *Cyclin D2* mRNA by *in-situ* hybridization (Supplementary Figure S6D–F', $n = 6$). Instead, strong expression of *Cyclin D2* mRNA was observed at the basal endfeet of the basally positioned daughter cell (Supplementary Figure S6F). As a control, *Ngn2* mRNA showed clear asymmetry between daughter cells and was more intense in the apically positioned daughter cell (Supplementary Figure S6G–I').

Disruption of Cyclin D2 asymmetry by acute overexpression or knockdown of gene expression distorts progenitor cell fate

If asymmetrical partitioning of Cyclin D2 protein among mitotic descendants is important for determining cell fate, then systemic alterations of Cyclin D2 levels in neuronal progenitor cells should be expected to disturb the output of asymmetric cell divisions. This would lead to distortions in the ratios of APs, IPs, and differentiated neurons. To induce overexpression of Cyclin D2, pCAX-Cyclin D2-ORF (or control pCAX) was constructed and electroporated in utero at E13.5 together with pCAX-EGFP-NLS (to visualize the nucleus). To knockdown Cyclin D2, si1726 or control siRNA was introduced into the E13.5 forebrain by *in-utero* electroporation together with pCAX-EGFP (Supplementary Figure S7A). Overexpression of Cyclin D2 (detectable as increased levels of mRNA and protein of Cyclin D2) in the VZ was clearly visible 24 h later in the vast majority of cells ($93.9 \pm 0.7\%$) present in the germinal zones ($n = 3$) (Supplementary Figure S7C, G and J). In comparison, cortices ($n = 3$) electroporated with control plasmid pCAX exhibited Cyclin D2 mRNA and protein in a smaller proportion of cells ($53.7 \pm 4.1\%$), representing endogenous levels of Cyclin D2 (Supplementary Figure S7B, F, and J; $P = 0.000346$). Conversely, knockdown of endogenous Cyclin D2 using si1726 produced a reduced number of Cyclin D2 immunopositive cells that was correlated with reduced *Cyclin D2* mRNA ($14 \pm 1.3\%$) (Supplementary Figure S7E, I, and J; $n = 3$). It is of note that Cyclin D2 mRNA and protein were diminished from the basal endfeet (Supplementary Figure S7E and inset of Supplementary Figure S7I). As expected, control siRNA electroporated into forebrains ($n = 3$) gave a similar proportion ($57.2 \pm 1.3\%$) of endogenously expressing Cyclin D2-positive cells and mRNA expression levels as pCAX control

(Supplementary Figure S7D, H and J; $P = 0.0000147$). We conclude that perturbing Cyclin D2, by overexpression or siRNA knockdown, is capable of disrupting the balance of Cyclin D2 leading to altered fates among daughter cells.

If differential Cyclin D2 levels in mitotic offspring can bias a cell towards a proliferative versus a differentiative fate, then altering Cyclin D2 levels on a global basis will be expected to change global ratios of cells with capacity for self-renewal (AP), further cell division but not renewal (IP), or fully differentiated (postmitotic neuron). Using markers to distinguish between these different cell types that coexist in the neuroepithelial wall, we quantified their relative frequency among EGFP-labelled cells that have become APs (Sox2 + / Tbr2 −), or IPs (Tbr2 +), or differentiated neurons (SOX2 −/ Tbr2 −) 24 h later (Supplementary Figure S7K–N). The results demonstrate that global overexpression of Cyclin D2 reduced the percentage of non-APs (marked by Tbr2 + or SOX2 −/ Tbr2 − immunostaining) ($53.1 \pm 1.7\%$ compared with $57.2 \pm 1.2\%$ in the control; $P = 0.0527$), but while at the same time increasing the percentage of APs (marked by SOX2 + /Tbr2 − staining) ($46.9 \pm 1.4\%$ compared with $42.6 \pm 1\%$ in the control; $P = 0.0527$) (Supplementary Figure S7O). On the other hand, loss-of-function experiment by RNAi knockdown led to increased percentage of neuronal cells (marked by Tbr2 + or SOX2 −/Tbr2 − immunostaining) ($63.9 \pm 0.4\%$ compared with $56.9 \pm 1.4\%$ in the control; $P = 0.01064$) at the expense of APs (SOX2 + /Tbr2 − immunostaining) ($36.1 \pm 0.4\%$ compared with $43.1 \pm 1.4\%$ in the control; $P = 0.01064$) (Supplementary Figure S7O). Thus, widespread expression of Cyclin D2 leads to the increased frequency of AP fates.

To further examine how cell fate was affected by perturbation of Cyclin D2 asymmetry in the longer term, the gain/loss of Cyclin D2 was performed at E12.5, and the location of the EGFP-reporter cells was analysed 48 h after *in-utero* electroporation. We found that overexpression of Cyclin D2 dramatically decreases in the percentage of EGFP + cells localized to the CP ($7.3 \pm 0.3\%$ compared with $15.3 \pm 0.2\%$ in the control; $P = 0.01069$), while at the same time increasing the percentage of EGFP + cells in the intermediate zone (IZ) and SVZ ($46.9 \pm 7.4\%$ compared with $37 \pm 0.7\%$ in the control; $P = 0.0541$) (Figure 6A, B, and E). In the loss-of-function experiment, the percentage of EGFP + cells localized to the CP was proportionally increased ($22.3 \pm 2.6\%$ compared with $15.4 \pm 0.3\%$ in the control; $P = 0.0519$) at the expense of the percentages in the VZ ($18 \pm 0.7\%$ compared with $20.2 \pm 1\%$ in the control; $P = 0.0535$) and SVZ ($18 \pm 2.7\%$ compared with $23.6 \pm 0.5\%$ in the control; $P = 0.0534$) (Figure 6C–E). Therefore, disruption of asymmetrical localization of Cyclin D2 perturbed normal differentiation of neural progenitor cells, while overexpression inhibited neuronal differentiation, loss-of-function promoted neuronal differentiation.

To confirm whether Cyclin D2 conversely promotes cell proliferation, BrdU was pulse labelled for 15 min before sampling. Compared with controls, a larger number of BrdU-labelled cells and mitotic marker PHH3-positive cells were present in the VZ of samples overexpressing Cyclin D2 (Supplementary Figure S8A, B, E, and F), indicating hyperproliferation of neural progenitor cells. Furthermore, ectopic BrdU-labelled cells and PHH3-positive cells were observed in the SVZ and IZ when *Cyclin D2* was overexpressed, implying that intermediate progenitors and subventricular radial
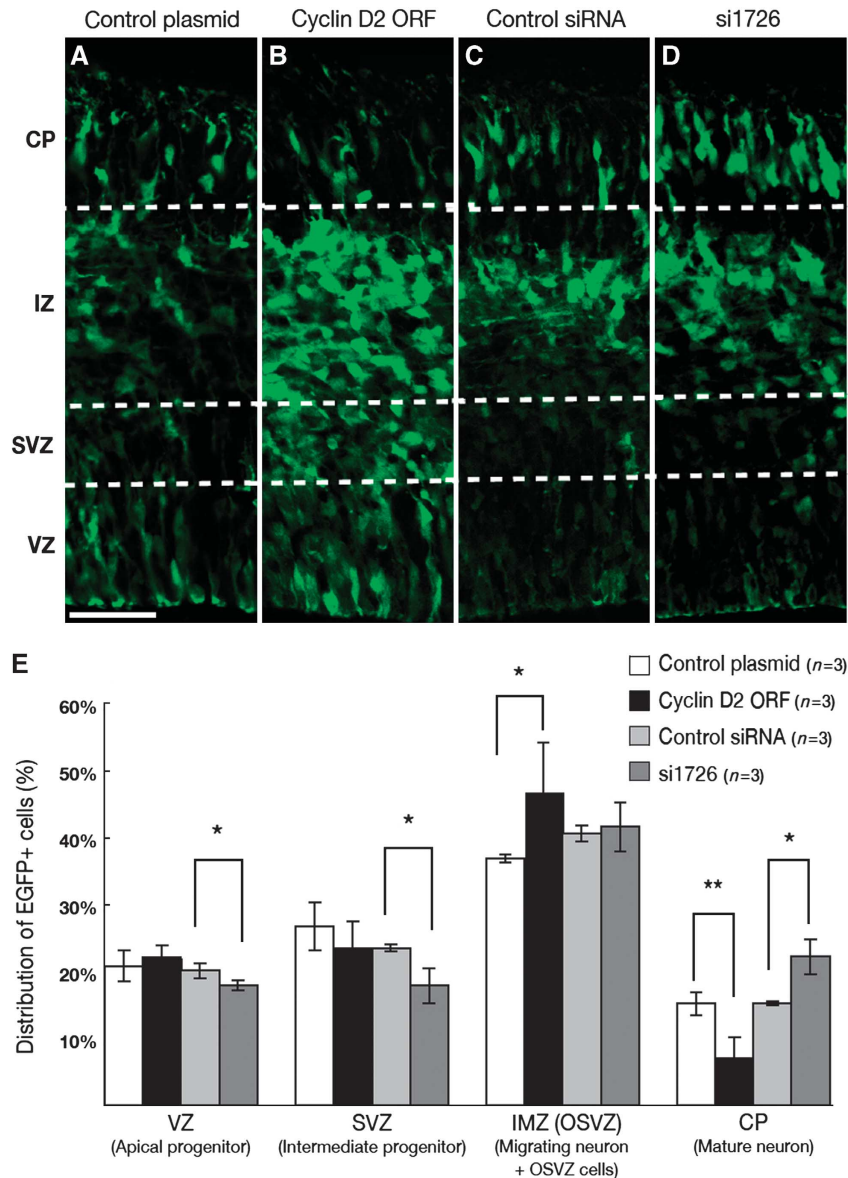
Figure 6 Alterations in cell position resulting from gain/loss of Cyclin D2. Cyclin D2 localization in cells expressing EGFP, 48 h after *in-utero* electroporation at E12.5 with control plasmid (*pCAX*), *pCAX-Cyclin D2-ORF*, control Stealth RNAi and Stealth RNAi for mouse *Cyclin D2* (si1726) together with *pCAX-EGFP*. Few EGFP + cells are observed in the CP of *pCAX-Cyclin D2-ORF*-electroporated samples (**B**) compared with control (**A**). In contrast, more EGFP + cells are observed in si1726-electroporated samples (**D**) than in controls (**C**) at CP. (**E**) Percentage of EGFP + cells in the ventricular zone (VZ), subventricular zone (SVZ) and intermediate zone/outer subventricular zone (IMZ/OSVZ) and cortical plate (CP). The VZ is identified as a Tbr2-negative zone and the SVZ identified as a Tbr2-positive zone (data not shown). IZ and CP were distinguished by their morphologies. Error bars indicate s.e.m. $*P < 0.05$, $**P < 0.01$, Student's *t*-test. Scale bar: 50 µm.

progenitors may undergone division in response to Cyclin D2 overexpression (Supplementary Figure S8A, B, E, and F). In contrast, downregulation of *Cyclin D2* dramatically decreased the number of BrdU-labelled cells and PHH3-positive cells in the VZ and the SVZ relative to controls (Supplementary Figure S8C, D, G, and H). These results confirm that Cyclin D2 is a very strong mitotic cue for neural progenitors.

We have demonstrated the inversely correlated expression patterns of Cyclin D2 and Ngn2 between daughter cells during cortical development (Figures 4N, 5M and N; Supplementary Figure S5). Moreover, the results obtained here revealed that loss of Cyclin D2 expression in the basally positioned daughter cells induced precocious neuronal differ-

entiation (Figure 6E; Supplementary Figure S7O). Thus, all these findings consistently suggest the importance of the asymmetrical distribution of Cyclin D2 protein in the AP cell; specifically, Cyclin D2-negative apical daughter cells will differentiate into neurons, while Cyclin D2-positive basally positioned daughter cells will take on a progenitor fate and proceed to cell division.

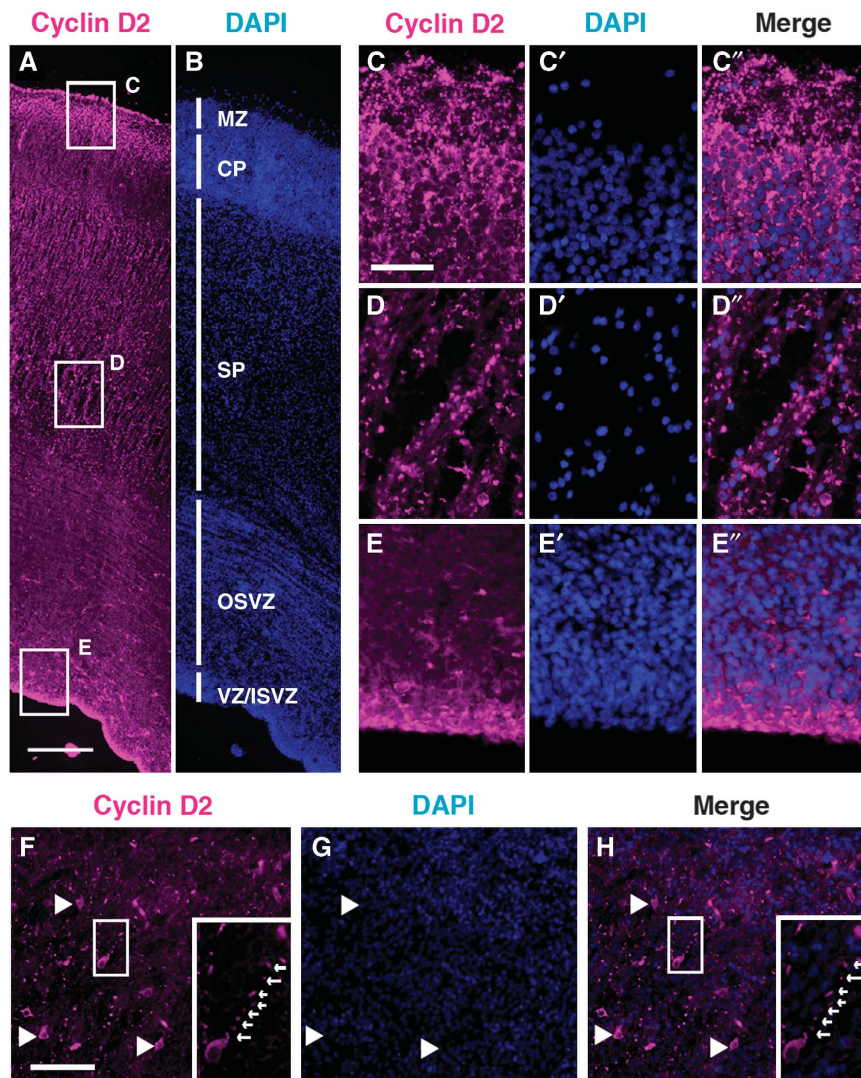### Cyclin D2 expression in the developing human cortex

If asymmetric Cyclin D2 partitioning to mitotic offspring is crucial for the determination of self-renewing fate, then one would expect this mechanism to be both ancient and conserved. Since it is not feasible to perform similar perturbation

experiments on human brains, we decided to compare Cyclin D2 protein localization in the human cortex. At 16 and 19 gestational weeks (GW), Cyclin D2 protein was strongly observed at the marginal zone (MZ) and upper part of CP (Figure 7A–C). Cyclin D2 protein was not localized in the nuclei of CP cells, but localized in the basal endfoot of the radial glia in upper CP and MZ (Figure 7C–C''). In the relatively expanded subplate (SP) of the human cortex, punctate Cyclin D2 localization was observed along the glial fibres (Figure 7D–D''). In the VZ and inner SVZ (ISVZ), Cyclin D2 expression was observed in the nucleus of radial glia (Figure 7E–E''). Therefore, the general pattern of Cyclin D2 in humans is remarkably similar to the rodent, suggesting the conservation of this mechanism. Moreover, recent studies have identified new sub-populations of proliferative cells in the outer SVZ in the fetal human and ferret brains; these cells are distinguished by their possession of basal but not apical processes (Fietz *et al*, 2010; Hansen *et al*,

2010). Examination of cortical tissue at 19 GW confirmed that Cyclin D2 was present in cells of the OSVZ, and in addition, also present in the basal process (Figure 7F–H, insets). At the genetic level, it is noteworthy that human *Cyclin D2* mRNA (NM-001759) also contains a predicted 50 bp transport element in the 3'UTR (with 74% sequence match to the mouse), raising the possibility that basal transport of human *Cyclin D2* mRNA for local translation in the basal process may also be operative.

Discussion

During corticogenesis, the cells that populate the expanding cortical wall comprise a heterogeneous mixture of dividing and non-dividing cells. This balance is necessary to ensure that the correct number of neurons are generated at an appropriate stage, and at the same time, maintaining a pool of self-renewing progenitors. To achieve this, progenitors

Figure 7 Cyclin D2 protein is expressed in the developing human cortex. (**A–E''**) At 16 GW, Cyclin D2 is expressed at three principal locations: the basal aspects of the CP near the MZ (box C); the subplate (box D), and the apical aspects of the VZ (box E). At higher magnification, Cyclin D2 in the basal aspects and the subplate are present in a punctate fashion along the cellular processes and not in the cell nuclei stained with DAPI (**C**, **D**). In the VZ, Cyclin D2 staining colocalizes with nuclei of neural progenitor cells (**E**). (**F–H**) Localization of Cyclin D2 protein in SP and OSVZ regions of the 19 GW human cortex showing Cyclin D2 staining in cells and also in a long basal process (**F** and **H**; arrows in insets). MZ, marginal zone; CP, cortical plate; SP, subplate; OSVZ, outer subventricular zone; VZ/ISVZ, ventricular zone/inner subventricular zone. Scale bars: 100 μm in (**A** and **B**), 25 μm in (**C–E''**), and 50 μm in (**F–H**).

undergo both symmetric and asymmetric cell divisions, but these events are classified by their outcomes rather than by their prior appearance or behaviour. While it is still not possible to forecast whether a progenitor will undergo symmetric or asymmetric division, a number of studies have attempted to link the mode of division with the acquisition of certain cellular and molecular characteristics. For example, cleavage plane orientation has been suggested to be a key factor (Chenn and McConnell, 1995; Zhong *et al*, 1996), but the low frequency of horizontal cleavage planes in the proliferative wall is irreconcilable with the large number of cortical neurons that needs to be produced (Huttner and Brand, 1997). While cleavage plane orientation is now considered to be unrelated to the mode of cell division (Attardo *et al*, 2008; Noctor *et al*, 2008), fate determinants such as Numb, present at the apical border, and TRIM32, present at the basal side of the cell body, appear to be preferentially inherited by the terminally differentiating daughter (Shen *et al*, 2002; Schwamborn *et al*, 2009). Other proteins found at the apical membrane, such as the Par complex (Costa *et al*, 2008; Bultje *et al*, 2009), have been implicated for controlling the balance between self-renewing and non-self-renewing divisions. By contrast, proteins enriched at the basal end of the progenitor have been less well studied as potential regulators of asymmetric versus symmetric cell division.

In this study, we revealed that allocation of Cyclin D2 to the tip of the basal process and its subsequent inheritance to the basally positioned daughter cell is strongly associated with the acquisition of a self-renewing fate of the AP. During mitosis the apically positioned daughter cell, expressing Ngn2, will adopt a different fate as a neuron or an IP (Figure 8). In summary, Cyclin D2 is expressed in the basal endfoot and nucleus, but by G1, it begins to be partitioned from the inherited basal process to the self-renewing daughter cell of the AP during an asymmetric division event. By late G1, asymmetric partitioning of Cyclin D2 becomes a hallmark for the basally positioned progenitor that is invariably nonneuronal (Ngn2 negative). Despite the first sign of Cyclin D2 asymmetry appearing in G1 pairs still attached to the apical surface, the majority of such daughter pairs either show equally weak Cyclin D2 distribution, or no Cyclin D2 whatsoever in both daughters. Interestingly, these daughter pairs rarely stain with Ngn2, suggesting the fate of each daughter cells remained uncommitted in this period.
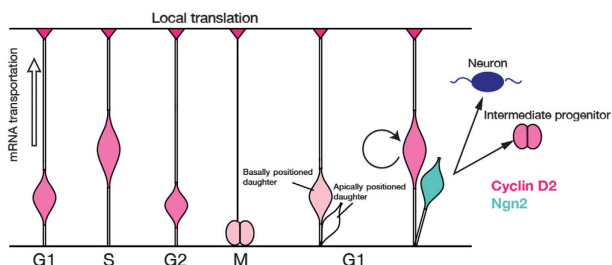
Figure 8 Schematic depiction of *Cyclin D2* mRNA and protein localization during the cell cycle and its putative role as a fate determinant. Pink and blue colours indicate Cyclin D2 and Ngn2 localization in the radial glia, respectively. *Cyclin D2* mRNA is transported to the basal endfoot during S-to-G2 phase (light pink arrow) and translated into protein. During mitosis, *Cyclin D2* mRNA or protein is inherited by the basally positioned daughter cell that assumes an apical progenitor fate.

If asymmetric distribution of Cyclin D2 is required for asymmetric cell fate determination, then Cyclin D2 overexpression should increase the frequency of symmetric cell divisions leading to increased numbers of APs, with concomitant reductions in numbers of differentiated neurons. These effects were observed with Cyclin D2 overexpression, and the opposite results obtained using RNAi knockdown experiments (Supplementary Figure S7O). Notably, this knockdown almost depleted mRNA and protein of Cyclin D2 from the endfeet, and produced a greater impact on the cell fate of neural progenitors compared with overexpression experiments. In summary, localization of Cyclin D2 in the basal endfoot has a critical role in the process of early corticogenesis.

An interesting aspect of Cyclin D2 is the strategy employed for unequal inheritance. Unlike Numb where the protein is preferentially allocated to the neuronal daughter (Shen *et al*, 2002), Cyclin D2 relies on transport of its mRNA during the S-to-G2 phase to the basal endfoot, where it is locally translated. This strategy relies on a 50-bp *cis*-acting transport element, present in full-length transcripts of *Cyclin D2* for translation into a 32-kDa protein (Denicourt *et al*, 2003), which is both necessary and sufficient for basal transport of fluorescent reporters. Importantly, this unique element is neither present in mouse *Cyclin D1* (Supplementary Figure S2) nor in chick *Cyclin D2* (NM-204213), both of which do not show asymmetric expression patterns in the developing forebrain. Sequence analysis of small RNAs do not exclude the possibility (Wang, 2008; Wang and El Naqa, 2008) that Cyclin D2 could be a potential target of certain microRNAs (e.g., mir-1192 and mir-495), but it remains unknown whether miRNA activity can be spatially distinctive enough to cause unequal distribution of *Cyclin D2* mRNA and protein in the endfoot. Moreover, a clear difference in Cyclin D2 protein levels between daughter cells is produced after cell division.

It has been mooted that inheritance of the basal process is associated with, and required for, asymmetric divisions (Konno *et al*, 2008). If that is correct, what then might be the mechanism that leads Cyclin D2 in the basal process to favour an AP fate? One possibility is that the long basal process increases the temporal interval for Cyclin D2 in the endfoot to gain access to the nucleus at G1. It is known that neural progenitors elongate their G1 phases during corticogenesis (Takahashi *et al*, 1995) and that progenitors at G1 are vulnerable to fate-determining events (McConnell and Kaznowski, 1991). Thus, delaying the interval of exposure to the nucleus by fate determinants such as Cyclin D2 may generate effects that are akin to shortening the G1 phase, thereby preventing the recipient nucleus from assuming a neuronal fate and favouring an AP fate. Indeed, artificial elongation of the G1 phase by another family protein, Cyclin D1, causes premature neurogenesis (Calegari and Huttner, 2003), while removal of Cyclin D2 gene by deletion causes G1 lengthening, leading to early exit from the cell cycle and encouraging neuronal differentiation (Glickstein *et al*, 2009). In that study, *Cyclin D2* knockout mice exhibit microcephaly and thinner cortical walls (Glickstein *et al*, 2009), features consistent with the present hypothesis that Cyclin D2 is crucial for maintaining divisions of APs.

In the present study, the increased focus on the basal process for AP fate has parallels in primates. In the outer

SVZ of human, ferret, and mouse cortices, a new population of proliferative cells have recently been reported to have basal processes but not apical processes and divide asymmetrically to produce one progenitor and one neuronal cell (Fietz *et al*, 2010; Hansen *et al*, 2010; Reillo *et al*, 2010; Wang *et al*, 2011). In addition, it has been reported that the basal process is instrumental for relaying a retinoic acid signal from the meninges to control progenitor cell proliferation (Siegenthaler *et al*, 2009). Given that we observe broad similarities in Cyclin D2 protein expression between developing mouse and human cortices, it is worth postulating that despite 70 million years of evolutionary divergence, the role of Cyclin D2 in maintaining AP renewal may be operative in all mammalian species. Furthermore, given its capacity to influence progenitor cell renewal, Cyclin D2 lends itself for evolutionary selection to increase the number of cell cycles (known to occur in primates) for generating a larger cortex (Finlay and Darlington, 1995; Rakic, 1995; Dehay and Kennedy, 2007), or within a given area of the cortex to generate more neurons for increased architectonic complexity (Dehay *et al*, 1993).

Materials and methods

Animals
Animal experiments were carried out in accordance with the National Institutes of Health Guide for the Care and Use of Laboratory Animals. The Committee for Animal Experimentation of the Tohoku University Graduate School of Medicine approved the experimental procedures described herein. The midday of the vaginal plug was designated as embryonic day 0.5 (E0.5). Pregnant ICR mice were purchased from Charles River Japan (Yokohama, Japan). *Cyclin D2* knockout mice were kindly obtained from Dr Sicinski (Sicinski *et al*, 1996).

Fetal tissue collection
Human fetal brain tissue was obtained from the NSW Fetal Tissue Consortium with approval from the University of Sydney Human Research Ethics Committee and the Melbourne Health Human Research Ethics Committee. This work was carried out under the NHMRC National Statement on Ethical Conduct in human research. Gestation age of fetus ranged between 16 and 19 weeks. Brain tissue was dissected and transported in ice-cold HEPES-buffered MEM (Invitrogen, Carlsbad, CA) and fixed in 4% paraformaldehyde (PFA) (w/v) in 0.1 M phosphate buffer (PB) for 1–9 h at 4°C. Fixed tissue was dehydrated in 20% sucrose in PB, embedded and frozen at −80°C in O.C.T compound (Tissue-Tek) and cryosectioned.

Staining procedures
In-situ hybridization and immunostaining procedures were performed according to methods previously described (Takahashi and Osumi, 2002). Antibodies used are listed in Supplementary Table 1. Information about probes, primers, and antibodies are supplied in Supplementary data.

Expression constructs
All expression constructs used in this study were cloned in frame into *pCAX* expression vector, a modified version of *pCAGGS*, in which multicloning site was inserted and the SV40 origin was deleted (kindly provided by the late K Umesono). All constructs were verified by sequence analysis. The entire mouse *Cyclin D2* cDNA (RIKEN MOUSE FANTOM, GenBank accession number

AK14745) was obtained from DANAFORM (Yokohama, Japan). For the *cis*-acting transport element assay, parts of the *Cyclin* D2 3′UTR sequence were subcloned into *pCAX-EGFP* downstream of the EGFP sequence.

Gene transfer into mouse embryos by electroporation
The experimental procedures for whole-embryo culture and electroporation have been described previously (Osumi and Inoue, 2001; Takahashi *et al*, 2008). The *pCAGGS-mRFP* vector was kindly provided by Dr Masanori Uchikawa. The *pCAX-Cyclin D2-ORF* was generated by the insertion of PCR-amplified ORF into the *pCAX* vector. The stealth RNAi against mouse *Cyclin D2* (*Si1726*, UUAGGUAGCAGCUACUUUAGUCAGC) and the scramble control RNAi (*SiCtr*, UUACUGGAUGCGACUCAUGAUUAGC) were purchased from Invitrogen and used in 200 µg/µl phosphate buffer saline (PBS) solution.

Virus production and injection into the brain
EGFP lentivirus was produced using *pCS-EF-EGFP*, *pCMV-VSV-G-RSV-Rev*, and *pCAG-HIVgp* plasmids, which were kindly provided by Dr Miyoshi as described previously (Tahara-Hanaoka *et al*, 2002). For details, see Supplementary data.

Statistical analysis
The quantitative data were evaluated by Student's *t*-test, using Excel 2004 for Mac (Microsoft, WA, USA), and presented as mean ± s.e.m.

Supplementary data
Supplementary data are available at *The EMBO Journal* Online (http://www.embojournal.org).

Conflict of interest

The authors declare that they have no conflict of interest.

References

Alexandre P, Reugels AM, Barker D, Blanc E, Clarke JD (2010) Neurons derive from the more apical daughter in asymmetric divisions in the zebrafish neural tube. *Nat Neurosci* **13**: 673–679

Astrom KE, Webster HD (1991) The early development of the neopallial wall and area choroidea in fetal rats. A light and electron microscopic study. *Adv Anat Embryol Cell Biol* **123**: 1–76

Attardo A, Calegari F, Haubensak W, Wilsch-Brauninger M, Huttner WB (2008) Live imaging at the onset of cortical neurogenesis reveals differential appearance of the neuronal phenotype in apical versus basal progenitor progeny. *PLoS One* 3: e2388

Bultje RS, Castaneda-Castellanos DR, Jan LY, Jan YN, Kriegstein AR, Shi SH (2009) Mammalian Par3 regulates progenitor cell asymmetric division via notch signaling in the developing neocortex. *Neuron* 63: 189–202

Calegari F, Huttner WB (2003) An inhibition of cyclin-dependent kinases that lengthens, but does not arrest, neuroepithelial cell cycle induces premature neurogenesis. *J Cell Sci* 116(Part 24): 4947–4955

Chenn A, McConnell SK (1995) Cleavage orientation and the asymmetric inheritance of Notch1 immunoreactivity in mammalian neurogenesis. *Cell* 82: 631–641

Costa MR, Wen G, Lepier A, Schroeder T, Gotz M (2008) Par-complex proteins promote proliferative progenitor divisions in the developing mouse cerebral cortex. *Development* 135: 11–22

Dehay C, Giroud P, Berland M, Smart I, Kennedy H (1993) Modulation of the cell cycle contributes to the parcellation of the primate visual cortex. *Nature* 366: 464–466

Dehay C, Kennedy H (2007) Cell-cycle control and cortical development. *Nat Rev Neurosci* 8: 438–450

Denicourt C, Kozak CA, Rassart E (2003) Gris1, a new common integration site in Graffi murine leukemia virus-induced leukemias: overexpression of a truncated cyclin D2 due to alternative splicing. *J Virol* 77: 37–44

Fietz SA, Kelava I, Vogt J, Wilsch-Brauninger M, Stenzel D, Fish JL, Corbeil D, Riehn A, Distler W, Nitsch R, Huttner WB (2010) OSVZ progenitors of human and ferret neocortex are epithelial-like and expand by integrin signaling. *Nat Neurosci* 13: 690–699

Finlay BL, Darlington RB (1995) Linked regularities in the development and evolution of mammalian brains. *Science* 268: 1578–1584

Glickstein SB, Alexander S, Ross ME (2007) Differences in cyclin D2 and D1 protein expression distinguish forebrain progenitor subsets. *Cereb Cortex* 17: 632–642

Glickstein SB, Monaghan JA, Koeller HB, Jones TK, Ross ME (2009) Cyclin D2 is critical for intermediate progenitor cell proliferation in the embryonic cortex. *J Neurosci* 29: 9614–9624

Gotz M, Huttner WB (2005) The cell biology of neurogenesis. *Nat Rev* 6: 777–788

Hansen DV, Lui JH, Parker PR, Kriegstein AR (2010) Neurogenic radial glia in the outer subventricular zone of human neocortex. *Nature* 464: 554–561

Haubensak W, Attardo A, Denk W, Huttner WB (2004) Neurons arise in the basal neuroepithelium of the early mammalian telencephalon: a major site of neurogenesis. *Proc Natl Acad Sci USA* 101: 3196–3201

Huttner WB, Brand M (1997) Asymmetric division and polarity of neuroepithelial cells. *Curr Opin Neurobiol* 7: 29–39

Huttner WB, Kosodo Y (2005) Symmetric versus asymmetric cell division during neurogenesis in the developing vertebrate central nervous system. *Curr Opin Cell Biol* 17: 648–657

Kamei Y, Inagaki N, Nishizawa M, Tsutsumi O, Taketani Y, Inagaki M (1998) Visualization of mitotic radial glial lineage cells in the developing rat brain by Cdc2 kinase-phosphorylated vimentin. *Glia* 23: 191–199

Konno D, Shioi G, Shitamukai A, Mori A, Kiyonari H, Miyata T, Matsuzaki F (2008) Neuroepithelial progenitors undergo LGN-dependent planar divisions to maintain self-renewability during mammalian neurogenesis. *Nat Cell Biol* 10: 93–101

Kosodo Y, Huttner WB (2009) Basal process and cell divisions of neural progenitors in the developing brain. *Dev Growth Differ* 51: 251–261

Kosodo Y, Roper K, Haubensak W, Marzesco AM, Corbeil D, Huttner WB (2004) Asymmetric distribution of the apical plasma membrane during neurogenic divisions of mammalian neuroepithelial cells. *EMBO J* 23: 2314–2324

Kosodo Y, Toida K, Dubreuil V, Alexandre P, Schenk J, Kiyokage E, Attardo A, Mora-Bermudez F, Arii T, Clarke JD, Huttner WB (2008) Cytokinesis of neuroepithelial cells can divide their basal process before anaphase. *EMBO J* 27: 3151–3163

Kriegstein A, Noctor S, Martinez-Cerdeno V (2006) Patterns of neural stem and progenitor cell division may underlie evolutionary cortical expansion. *Nat Rev Neurosci* 7: 883–890

Lange C, Huttner WB, Calegari F (2009) Cdk4/cyclinD1 overexpression in neural stem cells shortens G1, delays neurogenesis, and promotes the generation and expansion of basal progenitors. *Cell Stem Cell* 5: 320–331

McConnell SK, Kaznowski CE (1991) Cell cycle dependence of laminar determination in developing neocortex. *Science* 254: 282–285

Miyata T, Kawaguchi A, Okano H, Ogawa M (2001) Asymmetric inheritance of radial glial fibers by cortical neurons. *Neuron* 31: 727–741

Miyata T, Kawaguchi A, Saito K, Kawano M, Muto T, Ogawa M (2004) Asymmetric production of surface-dividing and non-surface-dividing cortical progenitor cells. *Development* 131: 3133–3145

Noctor SC, Flint AC, Weissman TA, Dammerman RS, Kriegstein AR (2001) Neurons derived from radial glial cells establish radial units in neocortex. *Nature* 409: 714–720

Noctor SC, Martinez-Cerdeno V, Ivic L, Kriegstein AR (2004) Cortical neurons arise in symmetric and asymmetric division zones and migrate through specific phases. *Nat Neurosci* 7: 136–144

Noctor SC, Martinez-Cerdeno V, Kriegstein AR (2008) Distinct behaviors of neural stem and progenitor cells underlie cortical neurogenesis. *J Comp Neurol* 508: 28–44

Ochiai W, Nakatani S, Takahara T, Kainuma M, Masaoka M, Minobe S, Namihira M, Nakashima K, Sakakibara A, Ogawa M, Miyata T (2009) Periventricular notch activation and asymmetric Ngn2 and Tbr2 expression in pair-generated neocortical daughter cells. *Mol Cell Neurosci* 40: 225–233

Osumi N, Inoue T (2001) Gene transfer into cultured mammalian embryos by electroporation. *Methods* 24: 35–42

Palacios IM, St Johnston D (2001) Getting the message across: the intracellular localization of mRNAs in higher eukaryotes. *Annu Rev Cell Dev Biol* 17: 569–614

Rakic P (1988) Specification of cerebral cortical areas. *Science* 241: 170–176

Rakic P (1995) A small step for the cell, a giant leap for mankind: a hypothesis of neocortical expansion during evolution. *Trends Neurosci* 18: 383–388

Reillo I, de Juan Romero C, Garcia-Cabezas MA, Borrell V (2010) A role for intermediate radial glia in the tangential expansion of the mammalian cerebral cortex. *Cereb Cortex* 21: 1674–1694

Ross ME, Carter ML, Lee JH (1996) MN20, a D2 cyclin, is transiently expressed in selected neural populations during embryogenesis. *J Neurosci* 16: 210–219

Salomoni P, Calegari F (2010) Cell cycle control of mammalian neural stem cells: putting a speed limit on G1. *Trends Cell Biol* 20: 233–243

Schwamborn JC, Berezikov E, Knoblich JA (2009) The TRIM-NHL protein TRIM32 activates microRNAs and prevents self-renewal in mouse neural progenitors. *Cell* 136: 913–925

Shen Q, Zhong W, Jan YN, Temple S (2002) Asymmetric Numb distribution is critical for asymmetric cell division of mouse cerebral cortical stem cells and neuroblasts. *Development* 129: 4843–4853

Sicinski P, Donaher JL, Geng Y, Parker SB, Gardner H, Park MY, Robker RL, Richards JS, McGinnis LK, Biggers JD, Eppig JJ, Bronson RT, Elledge SJ, Weinberg RA (1996) Cyclin D2 is an FSH-responsive gene involved in gonadal cell proliferation and oncogenesis. *Nature* 384: 470–474

Siegenthaler JA, Ashique AM, Zarbalis K, Patterson KP, Hecht JH, Kane MA, Folias AE, Choe Y, May SR, Kume T, Napoli JL, Peterson AS, Pleasure SJ (2009) Retinoic acid from the meninges regulates cortical neuron generation. *Cell* 139: 597–609

Smart IH (1973) Proliferative characteristics of the ependymal layer during the early development of the mouse neocortex: a pilot study based on recording the number, location and plane of cleavage of mitotic figures. *J Anat* 116(Part 1): 67–91

Tahara-Hanaoka S, Sudo K, Ema H, Miyoshi H, Nakauchi H (2002) Lentiviral vector-mediated transduction of murine CD34(-) hematopoietic stem cells. *Exp Hematol* 30: 11–17

Takahashi M, Nomura T, Osumi N (2008) Transferring genes into cultured mammalian embryos by electroporation. *Dev Growth Differ* 50: 485–497

Takahashi M, Osumi N (2002) Pax6 regulates specification of ventral neurone subtypes in the hindbrain by establishing progenitor domains. *Development* 129: 1327–1338

Takahashi M, Sato K, Nomura T, Osumi N (2002) Manipulating gene expressions by electroporation in the developing brain of mammalian embryos. *Differentiation* **70:** 155–162

Takahashi T, Nowakowski RS, Caviness Jr VS (1995) The cell cycle of the pseudostratified ventricular epithelium of the embryonic murine cerebral wall. *J Neurosci* **15:** 6046–6057

Wang X (2008) miRDB: a microRNA target prediction and functional annotation database with a wiki interface. *RNA* **14:** 1012–1017

Wang X, El Naqa IM (2008) Prediction of both conserved and nonconserved microRNA targets in animals. *Bioinformatics* **24:** 325–332

Wang X, Tsai JW, LaMonica B, Kriegstein AR (2011) A new subtype of progenitor cell in the mouse embryonic neocortex. *Nat Neurosci* **14:** 555–561

Zhong W, Feder JN, Jiang MM, Jan LY, Jan YN (1996) Asymmetric localization of a mammalian numb homolog during mouse cortical neurogenesis. *Neuron* **17:** 43–53